

CALL FOR PAPERS | *Translational Research in Acute Lung Injury and Pulmonary Fibrosis*

Rikkunshito ameliorates bleomycin-induced acute lung injury in a ghrelin-independent manner

AQ: 1

Hironobu Tsubouchi,¹ Shigehisa Yanagi,¹ Ayako Miura,¹ Seiichi Iizuka,² Sachiko Mogami,² Chihiro Yamada,² Tomohisa Hattori,² and Masamitsu Nakazato¹

¹Division of Neurology, Respiriology, Endocrinology and Metabolism, Department of Internal Medicine, Faculty of Medicine, University of Miyazaki, Kiyotake, Miyazaki, Japan; and ²Tsumura Research Laboratories, Tsumura, Ami-machi, Inashiki-gun, Ibaraki, Japan

Submitted 10 April 2013; accepted in final form 23 November 2013

AQ: 2

Tsubouchi H, Yanagi S, Miura A, Iizuka S, Mogami S, Yamada C, Hattori T, Nakazato M. Rikkunshito ameliorates bleomycin-induced acute lung injury in a ghrelin-independent manner. *Am J Physiol Lung Cell Mol Physiol* 306: L000–L000, 2014. First published November 27, 2013; doi:10.1152/ajplung.00096.2013.—Acute lung injury (ALI) is a critical syndrome consisting of acute respiratory failure associated with extensive pulmonary infiltrates. The pathological characterization of ALI includes injuries of alveolar epithelial cells (AECs), alveolar neutrophilic infiltration, and increases in proinflammatory cytokines, which cause destruction of the alveolar capillary barrier and subsequent devastating lung fibrosis. Rikkunshito (RKT), a traditional Japanese herbal medicine, is widely used for the treatment of patients with gastrointestinal symptoms and is known to stimulate ghrelin secretion. The therapeutic effects of RKT on organ inflammation and fibrosis remain unknown. We investigated the pharmacological potential of RKT in the treatment of ALI by using a bleomycin-induced ALI model in mice. RKT or distilled water (DW) was given to mice daily starting 12 h after bleomycin administration. The RKT-treated mice showed a definitively higher survival rate than the DW-treated mice after injury. They also had smaller reductions in body weight and food intake. The amelioration of neutrophil alveolar infiltration, pulmonary vascular permeability, induction of proinflammatory cytokines, activation of the NF- κ B pathway, apoptosis of AECs, and subsequent lung fibrosis were notable in the RKT-treated mice. RKT administration increased the plasma ghrelin levels in wild-type mice, and it also mitigated the ALI response in both ghrelin-deficient mice and growth hormone secretagogue receptor-deficient mice after lung injury. Our results indicate that RKT administration exerts protective effects against ALI by protecting the AECs and regulating lung inflammation independently of the ghrelin system, and they highlight RKT as a promising therapeutic agent for the management of this intractable disease.

rikkunshito; acute lung injury; ghrelin

ACUTE LUNG INJURY (ALI) and its severe clinical manifestation, acute respiratory distress syndrome (ARDS), constitute a devastating, life-threatening syndrome with a 60-day mortality rate of 26% (9). ALI/ARDS is physiologically characterized by extensive pulmonary infiltrates associated with severe arterial

hypoxia and impaired carbon dioxide excretion (51). The pathological characterization of ALI includes dysregulated inflammation consisting of increased proinflammatory cytokine levels, inappropriate leukocyte recruitment, and the uncontrolled activation of coagulation pathways (30, 31). The net result is injuries to the alveolar capillary barrier that lead to alveolar space flooding and subsequent devastating lung fibrosis (30–32). The alveolar epithelial cell (AEC) barrier shows a greater resistance to protein and fluid flux than the capillary endothelium (54), and the AECs are responsible for the active removal of fluid from the alveolar spaces (30). Indeed, damage to the endothelium alone is insufficient to cause pulmonary edema, whereas injury to the AECs results in severe lung injury (31). Protection of the integrity of AECs may therefore have a pronounced favorable effect on the control of ALI progression. Despite recent advances in understanding of the pathological mechanisms of ALI, the treatment strategies remain supportive in nature, and specific strategies to exert a protective effect on AECs have not been fully developed.

AQ: 3

Rikkunshito (RKT), a traditional Japanese herbal medicine, is widely prescribed to patients with various gastrointestinal symptoms, such as abdominal fullness, nausea, and postprandial early satiety (22). Previous studies showed that RKT ameliorated cisplatin-induced anorexia (43), suppressed 12-*O*-tetradecanoylphorbol-13-acetate-induced tumor promotion in mouse skin (60), and inhibited the apoptosis of small intestinal mucosal cells (44). However, the impact of RKT on the integrity of AECs and its therapeutic effects on organ inflammation and fibrosis, including in the lung, remain unknown.

Ghrelin is a 28-amino-acid peptide initially isolated from the human and rat stomach as an endogenous ligand for the growth hormone secretagogue receptor (19). In addition to its secretagogue action on growth hormone, ghrelin is known to have a broad array of actions including the promotion of food intake and anabolism (37), the suppression of inflammation (57), and the inhibition of apoptotic cell death (2, 26). We recently reported that ghrelin administration reduced lung inflammation, protected AECs, and ameliorated lung fibrosis in a bleomycin (BLM)-induced ALI model in mice (15). Another study indicated that RKT increased plasma ghrelin levels in healthy human volunteers and in normal mice (29). These findings prompted us to hypothesize that RKT would have a beneficial effect on ALI. In the present study, we investigated the efficacy

Address for reprint requests and other correspondence: H. Tsubouchi, Division of Neurology, Respiriology, Endocrinology and Metabolism, Dept. of Internal Medicine, Faculty of Medicine, Univ. of Miyazaki, Kiyotake, Miyazaki 889-1692, Japan (e-mail: hironobu_tsubouchi@med.miyazaki-u.ac.jp).

AQ: 4

of RKT administration on the amelioration of ALI using a BLM-induced ALI model in mice. We also tested whether RKT administration mitigates lung inflammation and subsequent lung fibrosis independently of the ghrelin system.

MATERIALS AND METHODS

Animals. Ten-week-old male C57BL/6N mice (wild-type mice) were purchased from Charles River Japan (Yokohama, Japan). Ten-week-old male ghrelin-deficient (*ghrl*^{-/-}) C57BL/6N mice (39) were generously provided by Dr. M. Kojima (Kurume University), and growth hormone secretagogue receptor-deficient (*ghsr*^{-/-}) C57BL/6N mice (41) were generously provided by Dr. Roy G. Smith (Baylor College of Medicine). Mice of both the wild-type (WT) and mutant strains weighed 22–29 g and were housed in a temperature-controlled room (23 ± 1°C) on a 12-h light (08:00–20:00):12-h dark cycle and fed a standard laboratory chow with ad libitum access to food. All experimental procedures were performed in accordance with the Japanese Physiological Society's guidelines for animal care and were approved by the University of Miyazaki Ethics Committee on Animal Experimentation.

Chemicals. BLM was obtained from Sigma-Aldrich Japan (Tokyo, Japan) and dissolved in sterile PBS. RKT (Tsumura, Tokyo, Japan) was made from a hot-water extract of a mixture of eight varieties of crude drugs [*Atractylodes lanceae rhizome* (4.0 g), *Ginseng radix* (4.0 g), *Pinelliae tuber* (4.0 g), *Hoelen* (4.0 g), *Zizyphi fructus* (2.0 g), *Aurantii nobilis pericarpium* (2.0 g), *Glycyrrhizae radix* (1.0 g), and *Zingiberis rhizome* (0.5 g)] and then spray dried. These medicinal plant materials were supplied through collection following cultivation in accordance with the World Health Organization guidelines on Good Agricultural and Collection Practices for medical plants (56). The quality of the resulting product satisfied the standards required by the Japanese Pharmacopoeia standards for herbal medicine. RKT, hesperidin, and glycyrrhizin (all obtained from Tsumura) were suspended in distilled water (DW) at the concentrations described below. Human ghrelin (Peptide Institute, Osaka, Japan) was dissolved in 200 µl of sterile PBS.

Administration of BLM and RKT. Mice were anesthetized by an intraperitoneal injection of pentobarbital sodium and were intratracheally administered 3 or 6 U/kg of BLM dissolved in 50 µl sterile PBS or 50 µl PBS. RKT (1,000 mg/kg), hesperidin, glycyrrhizin, or DW alone was administered orally by gavage, or ghrelin (10 nmol/mouse) was administered intraperitoneally starting 12 h after the BLM insult during the 3-day, 7-day, or 14-day study interval. We designated the BLM-injected, RKT-treated mice as the BLM/RKT group; the BLM-injected, ghrelin-treated mice as the BLM/ghrelin group; the BLM-injected, hesperidin-treated mice as the BLM/HES group; the BLM-injected, glycyrrhizin-treated mice as the BLM/GZ group; the BLM-injected, DW-treated mice as the BLM/DW group; the PBS-injected, RKT-treated mice as the PBS/RKT group; and the PBS-injected, DW-treated mice as the PBS/DW group, unless otherwise noted.

For the histological assay, we studied the PBS/DW group of WT mice ($n = 5$), *ghrl*^{-/-} mice ($n = 5$), and *ghsr*^{-/-} mice ($n = 5$), and we examined the animals on *day 0*. For the survival study, we used the BLM/RKT group ($n = 35$) and BLM/DW group ($n = 35$) using WT mice, the BLM/RKT group ($n = 21$) and BLM/DW group ($n = 2$ – 12) using *ghrl*^{-/-} mice, and the BLM/RKT group ($n = 23$) and BLM/DW group ($n = 23$) using *ghsr*^{-/-} mice. We monitored all groups for 14 days and recorded their survival. For the immunohistochemical analyses and terminal deoxynucleotidyl transferase-mediated dUTP nick-end labeling (TUNEL) assay, we used the BLM/RKT group and BLM/DW group ($n = 5$ per group of WT mice) and examined the animals on *days 0, 3, and 7*. We used the groups of BLM/RKT, BLM/DW, PBS/RKT, and PBS/DW for the histological assay ($n = 5$ per group of WT mice), bronchoalveolar lavage (BAL) ($n = 6$ – 11 per group of WT mice, $n = 3$ – 10 per group of *ghrl*^{-/-} mice, and $n =$

3 – 11 per group of *ghsr*^{-/-} mice), the lung wet-to-dry weight ratio ($n = 3$ – 12 per group of WT mice), an ELISA ($n = 3$ – 12 per group of WT mice), quantitative reverse transcription PCR (qRT-PCR) ($n = 3$ – 6 per group of WT mice), and immunoblotting ($n = 3$ – 4 per group of WT mice) and examined them on *day 7*. Body weights were measured daily from 1 day before BLM or PBS administration to *day 14*. The 14-day food intake amounts were also measured. For the measurements of body weights and food intake ($n = 7$ – 21 per group of WT mice, $n = 7$ – 16 per group of *ghrl*^{-/-} mice, $n = 5$ – 18 per group of *ghsr*^{-/-} mice), the modified Sircol collagen assay ($n = 5$ – 11 per group of WT mice, $n = 4$ – 11 per group of *ghrl*^{-/-} mice, and $n = 5$ – 12 per group of *ghsr*^{-/-} mice), histological assay ($n = 5$ per group of WT mice), and qRT-PCR ($n = 3$ – 11 per group of WT mice), we used four additional groups and examined the animals on *day 14*. For the modified Sircol collagen assay using the samples of post treatment of RKT, we used the BLM/RKT group ($n = 8$) and BLM/DW group ($n = 8$) using WT mice which were administered RKT or DW 7 days after a BLM (3 U/kg) injection, and we examined the animals on *day 21*. For the measurements of plasma ghrelin levels under the pair-fed condition, we used a BLM/DW group ($n = 4$), a BLM/RKT group ($n = 6$), and a BLM/ghrelin group ($n = 4$), all of which were administered 6 U/kg of BLM or PBS, and we examined them on *day 14*. For the qRT-PCR, we used BLM/DW group ($n = 6$) and BLM/RKT group ($n = 6$), both of which were administered 6 U/kg of BLM, and examined them on *day 14*. To evaluate the dose-dependent effect of RKT on the body weight change of BLM-injected mice, we used two different types of BLM/RKT groups that were administered 500 mg ($n = 17$) or 1,000 mg ($n = 15$) of RKT: a BLM/DW group ($n = 17$) and a PBS/DW group ($n = 17$). All groups were previously administered 6 U/kg of BLM. Body weights were measured daily from 1 day before BLM or PBS administration to *day 7*. To evaluate the dose-dependent effects of hesperidin and glycyrrhizin on the lung permeability in mice injected with 6 U/kg of BLM, we used three different BLM/HES and BLM/GZ dose groups in WT mice that were administered 10 ($n = 7$), 50 ($n = 7$), or 250 ($n = 7$) mg/kg of hesperidin and 25 ($n = 7$), 50 ($n = 7$), or 100 ($n = 8$) mg/kg of glycyrrhizin, and two BLM/DW groups of WT mice ($n = 7$ and 8). The timeline of the experimental schedule is given in Fig. 1.

F1

BAL. Mice were anesthetized 7 days after BLM injection, and the trachea was cannulated with a 20-gauge catheter. BAL with 1.0 ml of sterile PBS using a trachea tube was repeated five times. The collected bronchoalveolar lavage fluid (BALF) was centrifuged at 1,000 rpm for 5 min, and the supernatant was stored at -70°C until used. The cell pellet was used to determine the number of cells. Total BAL cells were enumerated by counting on a hemocytometer in the presence of Türk's solution (Merck, Tokyo, Japan). Cytospins were prepared from resuspended BAL cells. Cytospins of BAL cells were made by centrifuging 100,000 cells onto microscope slides with a Cytospin 4 (Thermo Fisher Scientific, Yokohama, Japan). Slides were allowed to air dry and were then stained with a Diff-Quik stain kit (Sysmex, Kobe, Japan). Cell differentials were determined by counting 300 cells under $\times 400$ magnification. The amount of total protein in the BALF supernatant was measured by the Bradford assay (1).

Wet-to-dry ratio of lung. The lungs were removed and weighed (wet lung weight) at 7 days after PBS or BLM injection. After 72 h of drying in an oven at 70°C , the lungs were weighed again (dry lung weight), and the ratio between the wet and dry lung weights was determined for each lung.

Measurement of the cytokine and chemokine levels in BALF. An ELISA was run using the BALF samples to measure the concentrations of IL-1 β , TNF- α , chemokine (C-X-C motif) ligand 2/macrophage inhibitory protein-2 (CXCL2/MIP2), and transforming growth factor- β_1 (TGF- β_1) by using the commercially available ELISA kits specifically designed for each protein (R&D Systems, Minneapolis, MN) according to the manufacturer's instructions.

Measurement of lung collagen levels. The lung collagen levels were assessed by a modified Sircol collagen protocol with sample

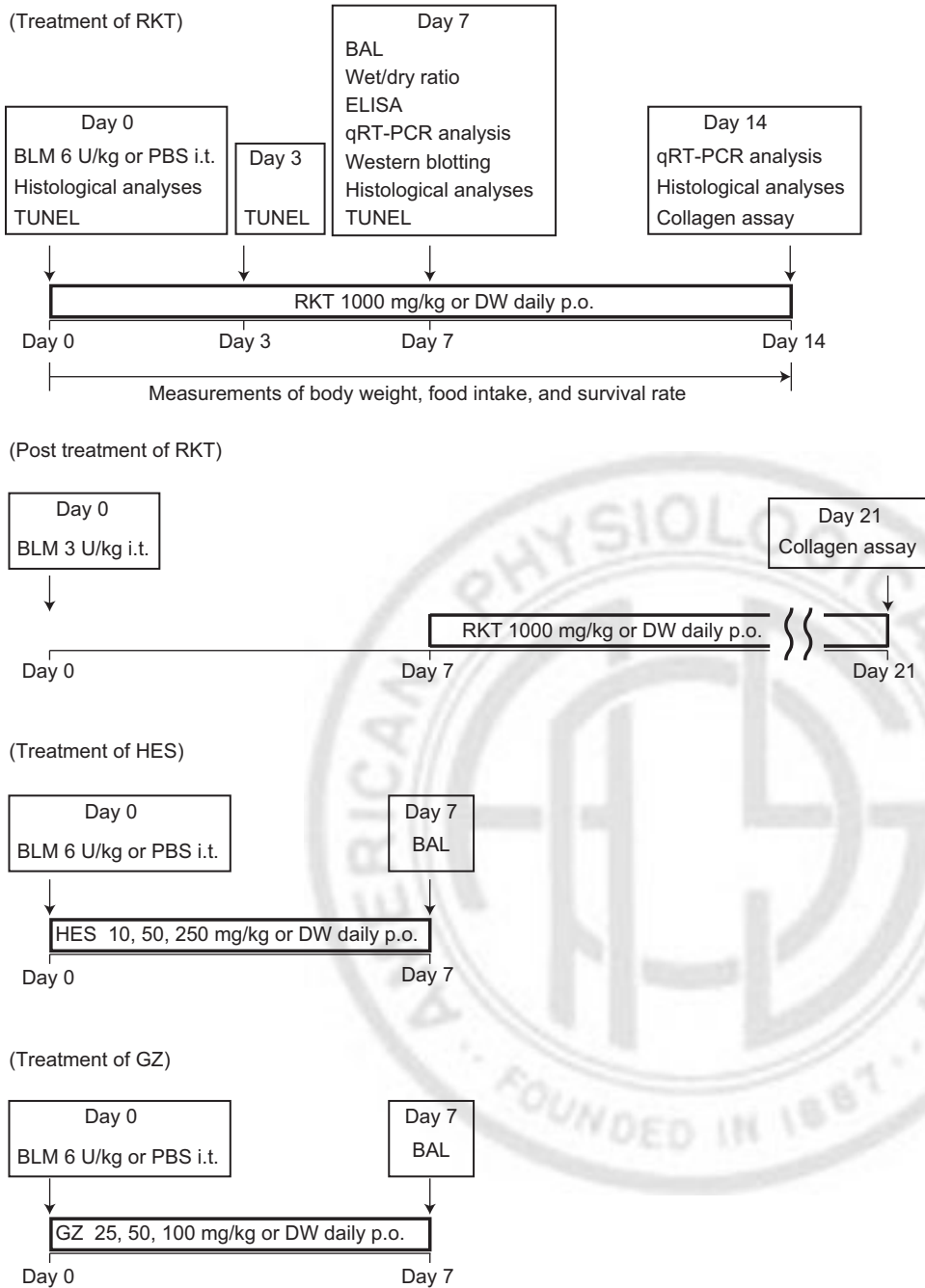


Fig. 1. Experimental schedule. DW, distilled water; BLM, bleomycin; RKT, rikkunshito; HES, hesperidin; GZ, glycyrrhizin; qRT-PCR, quantitative reverse transcription PCR; TUNEL, terminal deoxynucleotidyl transferase-mediated dUTP nick-end labeling; BAL, bronchoalveolar lavage; i.t., intratracheal administration; p.o., oral administration.

purification for the removal of interfering noncollagenous proteins as described (23). Briefly, mice were anesthetized 14 days after BLM or PBS injection, and lungs were removed, washed with cold PBS, frozen in liquid nitrogen, and stored at -70°C until used. The lung samples were homogenized in 1 ml of 0.5 M acetic acid solution by a TissueLyser II (Qiagen, Hilden, Germany). The homogenate samples were mixed 4 ml of 0.5 M acetic acid solution and pepsin (0.1 mg/ml), incubated overnight at 4°C , and centrifuged at $13,000\text{ g}$ for 10 min. For sample purification after pepsin digestion, an Amicon Ultra-0.5 Centrifugal Filter Unit with an Ultracel-100 kDa membrane (Merck, Tokyo, Japan) was used. Following pepsin treatment, the supernatants of the samples were loaded onto the columns and centrifuged at $13,000\text{ g}$ for 10 min. The retentate was then washed three times in dilute acetic acid (0.5 M) and recovered by the inversion of the filter insert and centrifugation. The filtrates were used for the

measurement of soluble collagen. Total lung collagen levels were determined by measuring soluble collagen in the lungs with a Sircol collagen assay kit (Biocolor, Carrickfergus, UK) according to the manufacturer's instructions.

Histological and immunohistochemical analyses and TUNEL assay. The lungs were fixed in 10% buffered formalin solution or Amsterdam's fixative (methanol-acetone-acetic acid-water, 35:35:5:25 vol/vol) and embedded in OCT compound (Sakura Finetek Japan, Tokyo, Japan). Lung sections ($4\text{ }\mu\text{m}$ thickness) were mounted on slides for hematoxylin-eosin (HE) and Masson's trichrome staining (Diagnostic BioSystems, Pleasanton, CA) and for immunostaining with an antibody recognizing surfactant protein-C (SP-C; Santa Cruz Biotechnology, Santa Cruz, CA). To evaluate the apoptosis of AECs, we performed a TUNEL assay of SP-C-immunostained lung tissue sections using an in situ cell death detection kit, TMR Red (Roche

Diagnosics, Basel, Switzerland). The sections were counterstained with 4'-6-diamidino-2-phenylindole (DAPI; Wako, Saitama, Japan). Ten high-power fields per slide were randomly selected, and the numbers of TUNEL-positive cells, SP-C-positive cells, and DAPI-positive cells were counted. For the quantification of colocalized cells from double-immunostained slides in the TUNEL assay, one investigator took photos of 10 random fields in a blinded fashion (i.e., without knowledge of which experimental or control groups the samples were taken from), and the cells in each field were counted independently by two other investigators in a blinded fashion. The percentages of TUNEL-positive cells and TUNEL and SP-C double-positive cells were obtained by dividing the number of TUNEL-positive cells by the number of DAPI-positive cells and by dividing TUNEL and SP-C double-positive cells by SP-C positive cells, respectively.

Measurement of plasma ghrelin levels and ghrelin mRNA levels in stomachs and lungs in BLM-injected mice. At 14 days after the BLM or PBS injection, blood was taken from the mice by heart puncture and collected in a tube that contained aprotinin and ethylenediaminetetraacetic acid (Wako, Osaka, Japan). It was stirred well and immediately centrifuged at 4°C. After plasma collection, a 1/10 volume of 1 mol/l HCl was added. The prepared plasma was stored at -80°C until the measurement of ghrelin. The plasma ghrelin assay is a two-site immunoenzymometric assay requiring 100 µl of plasma sample, which is performed automatically by an AIA-600II immunoassay analyzer (Tosoh, Tokyo, Japan). The stomachs and lungs were isolated 14 days after the BLM injection, preserved in RNA-later (Ambion, Austin, TX), and stored at -20°C until the analysis.

Extraction of mRNA and qRT-PCR. The extractions of mRNA from the whole lung tissues and the stomachs were performed with a RiboPure Kit (Life Technologies Japan, Tokyo, Japan). First-strand cDNA was generated by reverse transcription by use of a High Capacity RNA-to-cDNA Kit (Life Technologies Japan). We conducted a qRT-PCR using Taqman Fast Universal PCR Master Mix (Life Technologies Japan) and a Thermal Cycler Dice Real Time System II (Takara Bio, Tokyo, Japan). The levels of mRNA were determined by using cataloged primers (Applied Biosystems, Foster City, CA) for mice (IL-1β, Mm00434228_m1; IL-6, Mm00446190_m1; CXCL2, Mm00436450_m1; TGF-β₁, Mm01178820_m1; Collagen1a1, Mm00801666_g1; Collagen3a1, Mm01254476_m1; and ghrelin, Mm00445450_m1). The expression of these genes was normalized to the expression of hypoxanthine guanine phosphoribosyl transferase (HPRT) mRNA (HPRT: Mm01545399_m1) or glyceraldehyde-3-phosphate dehydrogenase (GAPDH) mRNA (GAPDH: Mm99999915_g1), and the results are expressed as relative fold differences.

Western blotting. We extracted cytoplasmic and nuclear proteins from whole lung tissues by NE-PER Nuclear and Cytoplasmic Extraction Reagents (Thermo Fischer Scientific, Yokohama, Japan). The cytoplasmic extracts and nuclear extracts were transferred to a new prechilled tube and stored at -70°C until used. The protein contents of the cytoplasmic extracts and the nuclear extracts were determined by a Bradford assay. Equal amounts of cytoplasmic and nuclear proteins were fractionated by 10% SDS-PAGE and transferred to Immobilon Transfer Membranes (Merck, Tokyo, Japan). We analyzed the extracts by Western blotting using antibodies recognizing the following proteins: IκBα, NF-κB p65, phosphorylated NF-κB p65, lamin A/C (Cell Signaling Technology Japan, Tokyo, Japan) and β-actin (Sigma-Aldrich Japan). To quantify protein expression, we used densitometry and Gene Tools software (Syngene, Frederick, MD) on the lanes.

Statistical analysis. All results are expressed as means ± SE. Data were analyzed by a one-way analysis of variance (ANOVA) followed by Dunnett's multiple comparison test. A *t*-test was used for comparisons between groups. Statistical analyses were done with JMP 10 (SAS Institute Japan, Tokyo, Japan). Kaplan-Meier survival analysis was performed with Prism 5 (GraphPad Software, La Jolla, CA), and

statistical significance was determined by log-rank test. *P* values < 0.05 were considered significant.

RESULTS

RKT administration attenuated the mortality, weight loss, and suppression of food intake in the BLM-injected mice. We first assessed the safety of the RKT administration. All of mice of both the PBS/DW and PBS/RKT groups (*n* = 12 per group) survived during the 14-day interval (data not shown). To explore the effect of RKT administration, we performed a survival study on a mouse model of ALI induced by the instillation of BLM. The survival rate of the BLM/DW group was 54% (19/35) on *day 14* (Fig. 2A). In contrast, RKT administration maintained a survival rate of 80% (28/35) on *day 14*. Kaplan-Meier analysis showed that the overall survival rate of the BLM/RKT mice was significantly higher than that of the BLM/DW group (log-rank, *P* = 0.018, Fig. 2A). We also analyzed the effects of RKT on body weight changes and food intake in the four groups with different experimental conditions. Intratracheal administration of BLM significantly decreased the body weights and food intake compared with the PBS groups (Fig. 2, B and C). The quantity of food intake and change in body weight during the 14-day experiment were not significantly different among the PBS-treated groups. In the BLM-treated groups, RKT administration significantly attenuated the weight loss and reduction of food intake (Fig. 2, B and C). RKT administration mitigated the loss of body weights of BLM-injected mice in a dose-dependent manner (Fig. 2D).

RKT administration reduced neutrophil alveolar infiltration, vascular permeability, levels of proinflammatory cytokines, and activation of the NF-κB signaling pathway in BLM-injected mice. At *day 7*, the lungs of the BLM/DW mice exhibited extensive infiltrations of inflammatory cells in the alveolar spaces compared with the PBS/DW lungs (Fig. 3A, left). RKT administration did not affect the histological findings of the lungs in the PBS groups (Fig. 3A, top). RKT administration to the BLM group reduced the intra-alveolar accumulation of inflammatory cells (Fig. 3A, bottom). BLM treatment significantly increased the numbers of total cells and neutrophils in the BALF of the DW groups (Fig. 3B). RKT administration significantly diminished these parameters in the BLM groups. The total protein concentrations in the BALF and the lung wet-to-dry weight ratios of the BLM group were higher than those in the PBS groups (Fig. 3, C and D). RKT administration significantly reduced these values after lung injury. In the BLM group, the concentrations of IL-1β, TNF-α, CXCL2/MIP2, and TGF-β₁ in the BALF were significantly higher than those in the PBS groups (Fig. 3E). RKT treatment reduced the levels of cytokines and chemokines in the BLM group. The levels of mRNA of IL-1β, IL-6, CXCL2/MIP2, and TGF-β₁ in the lysates of whole lung extracts were increased in the BLM groups compared with the PBS groups (Fig. 3F). These values in the BLM/RKT group were significantly lower than those of the BLM/DW group.

We next examined the effect of RKT administration on NF-κB activation in the lung tissue. The levels of nuclear and cytoplasmic NF-κB p65 protein and cytoplasmic phosphorylated NF-κB p65 protein of the BLM groups were higher than those of the PBS groups (Fig. 3G). RKT administration decreased all of these values after lung injury. The lung lysates

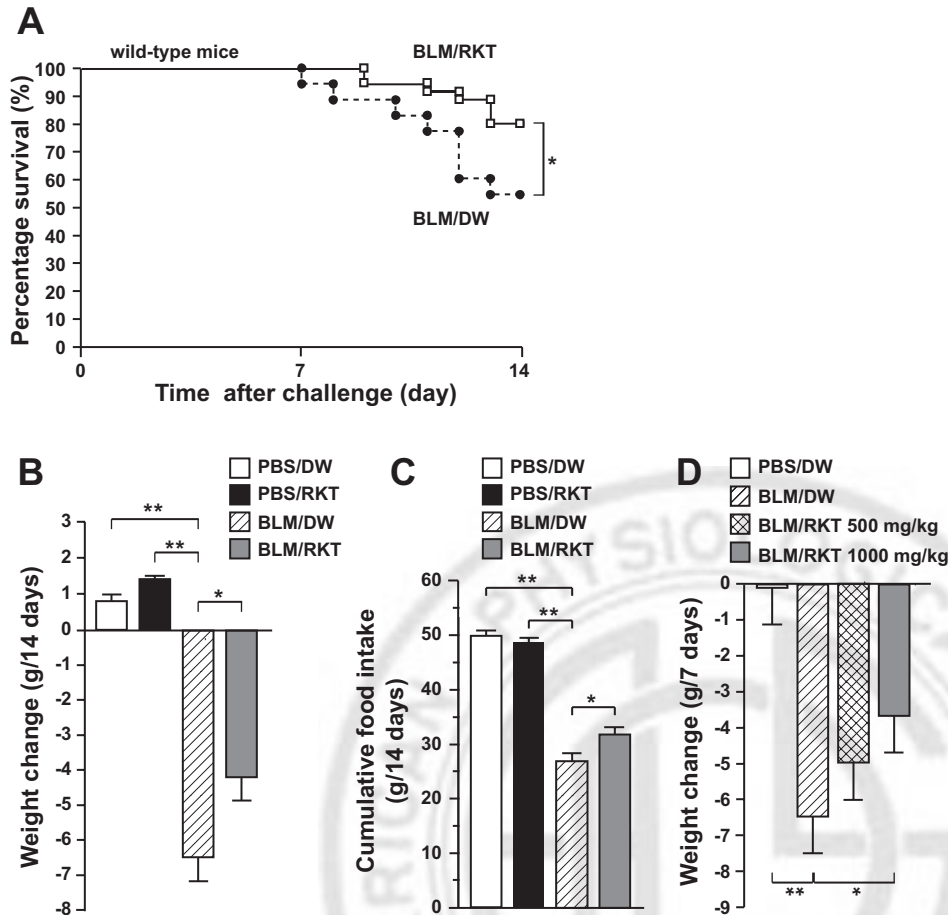


Fig. 2. Effects of RKT administration on survival rate, weight change, and food intake in BLM-injected mice. A: Kaplan-Meier survival curves for the BLM/DW group ($n = 35$, dashed line) and BLM/RKT group ($n = 35$, solid line) for 14 days after challenge with 6 U/kg of BLM. $*P < 0.05$. Alterations in body weight (B) and cumulative food intake (C) over 14 days after instillation of 6 U/kg of BLM or PBS are shown (PBS/DW $n = 7$, PBS/RKT $n = 7$, BLM/DW $n = 16$, BLM/RKT $n = 21$). D: alterations in the body weight of DW- and RKT-treated mice over 7 days after the instillation of 6 U/kg of BLM or PBS are shown (PBS/DW $n = 17$, BLM/DW $n = 17$, BLM/RKT 500 mg/kg $n = 17$, and BLM/RKT 1,000 mg/kg $n = 15$). Data are shown as means \pm SE. $*P < 0.05$; $**P < 0.01$.

isolated from BLM/DW mice showed decreased expression levels of cytoplasmic I κ B α compared with those of the PBS/DW mice. RKT treatment restored the expression of cytoplasmic I κ B α in the lung tissue after the BLM insult.

RKT administration reduced the BLM-induced lung fibrosis. We next evaluated the effects of RKT administration on lung fibrosis. At day 14, the lung sections from the BLM/DW mice showed extensive lung fibrosis associated with destruction of the normal lung architecture (Fig. 4A). In contrast, the lungs of the BLM/RKT mice demonstrated an amelioration of lung fibrosis and comparatively preserved lung architecture. Masson's trichrome staining showed dense collagen deposition in the BLM/DW mice, whereas the fibrotic changes were reduced in the BLM/RKT mice (Fig. 4A). The Sircol assay revealed a significant reduction of collagen contents in the BLM/RKT lungs compared with the BLM/DW lungs (Fig. 4B). The mRNA expressions of collagen type I α 1 and type III α 1 in the BLM/RKT group were significantly lower than those of the BLM/DW group (Fig. 4, C and D). RKT treatment 7 days after BLM administration also decreased the deposition of collagen contents in the lung tissue (Fig. 4E).

RKT administration suppressed the apoptosis of AECs in the BLM-injected mice. We used TUNEL staining to detect the apoptotic cells in the lung tissue. At day 3 and day 7, TUNEL-positive cells in the alveolar wall (predominantly comprised of apoptotic-type I AECs, type II AECs, endothelial cells, and fibroblasts) and TUNEL-SP-C double-positive cells (apoptotic-type II AECs) were frequently detected in the lung sections of

BLM/DW mice, whereas these cells were significantly decreased in the BLM/RKT mice (Fig. 5, A and B).

RKT administration attenuated the BLM-induced ALI independently of the ghrelin system. The administration of RKT significantly elevated the plasma concentrations of both ghrelin and des-acyl ghrelin and the ghrelin mRNA expression in the stomachs in the bleomycin groups (Fig. 6, A–C). The ghrelin mRNA levels in the lung tissues were comparable between the RKT-treated mice and the DW-treated mice after lung injury (Fig. 6D), probably because of the substantially lower expression amounts of ghrelin in the lung tissue compared with the counterparts of the stomach (13). The intraperitoneal administration of ghrelin overwhelmingly increased the plasma levels of ghrelin and des-acyl ghrelin in BLM-injected mice compared with the BLM/DW mice (Fig. 6, A and B).

To determine whether the ameliorative effects of RKT administration on BLM-induced 1) ALI responses and 2) decreases in food intake and body weight loss were due to direct effects of RKT or indirect mechanisms via its contribution to the induction of ghrelin secretion and/or the agonistic effect on growth hormone secretagogue receptor, we examined the effects of RKT administration by using the *ghrl*^{-/-} and *ghsr*^{-/-} mice. The histological appearances of the lung tissues in the C57BL/6, *ghrl*^{-/-}, and *ghsr*^{-/-} mice were similar before BLM administration (Fig. 7). The survival rate of the BLM/DW group was 50% (11/22) in the *ghrl*^{-/-} mice and 52% (12/23) in the *ghsr*^{-/-} mice at 14 days after BLM

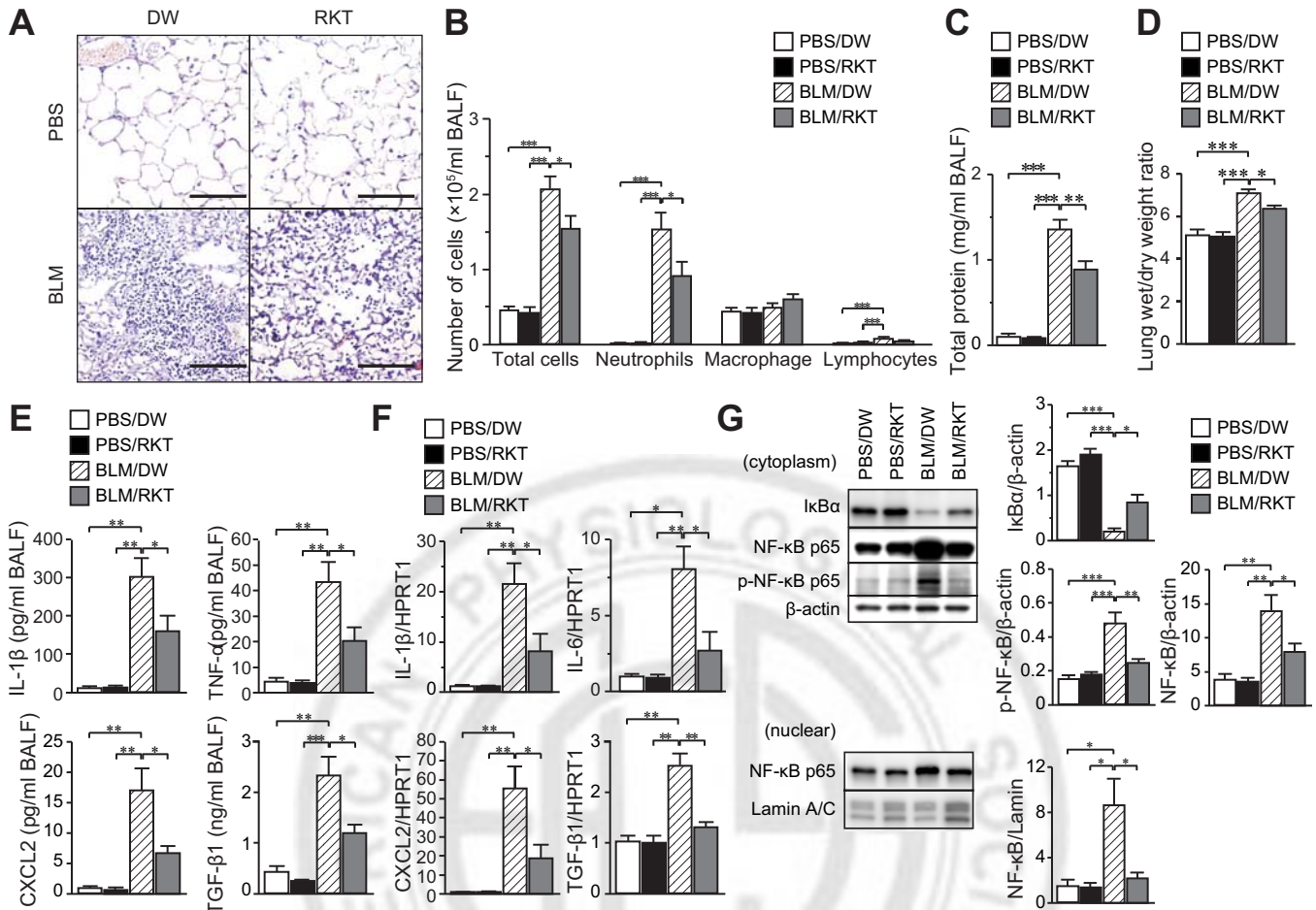


Fig. 3. Effects of RKT administration on neutrophil alveolar infiltration, vascular permeability, levels of proinflammatory cytokines, and NF-κB activation in BLM-injected mice. **A:** representative hematoxylin-eosin (HE) staining of lung sections of DW-administered (*left*) and RKT-administered (*right*) mice after treatment with PBS (*top*) or 6 U/kg of BLM (*bottom*). Data shown are representative lung sections from 5 mice per group. Scale bars: 100 μm. Cell counts (**B**) and total protein concentrations (**C**) in the bronchoalveolar lavage fluid (BALF) and lung wet-to-dry weight ratio (**D**) of DW- or RKT-administered mice 7 days after the instillation of PBS or 6 U/kg of BLM. Data are means ± SE of 6–11 (**B**), 5–7 (**C**), and 3–12 (**D**) mice per group. **P* < 0.05; ***P* < 0.01; ****P* < 0.001. **E:** concentrations of IL-1β, TNF-α, chemokine (C-X-C motif) ligand 2 (CXCL2), and transforming growth factor-β₁ (TGF-β₁) in the BALF. Data are means ± SE of 3–12 mice per group. **P* < 0.05; ***P* < 0.01; ****P* < 0.001. **F:** mRNA levels of IL-1β, IL-6, CXCL2, and TGF-β₁ in the whole lung lysates of DW- or RKT-administered mice 7 days after the instillation of PBS or 6 U/kg of BLM. Results are expressed relative to the housekeeping gene hypoxanthine phosphoribosyltransferase 1 (HPRT1). Data are means ± SE of 3–6 mice per group. **P* < 0.05; ***P* < 0.01. **G:** immunoblots of NF-κB p65 protein in the nucleus and phosphorylated NF-κB p65 protein, NF-κB p65 protein, and IκBα protein in the cytoplasm in the lysates of whole lung tissue from DW- or RKT-administered mice 7 days after administration of PBS or 6 U/kg of BLM. The quantitative comparisons were performed with lamin A/C and β-actin as loading controls. Data are means ± SE of 3–4 mice per group. **P* < 0.05; ***P* < 0.01; ****P* < 0.001.

F8 instillation (Figs. 8A and 9A). The RKT administration resulted in the survival rates of 81% (17/21) in the *ghrl*^{-/-} mice and 78% (18/23) in the *ghsr*^{-/-} mice after lung injury. Kaplan-Meier analysis showed that the survival rates of the BLM/RKT groups of *ghrl*^{-/-} mice and *ghsr*^{-/-} mice were significantly higher than those of corresponding BLM/DW groups (log-rank, *P* = 0.033 in *ghrl*^{-/-} mice, Fig. 8A, and *P* = 0.045 in *ghsr*^{-/-} mice, Fig. 9A). The administration of RKT did not decrease the degree of loss of body weight and food intake reduction in both the *ghrl*^{-/-} mice and *ghsr*^{-/-} mice after lung injury (Figs. 8B and 9B). In contrast to the effects on food intake and body weight changes, the RKT administration significantly inhibited the neutrophil alveolar infiltration, the protein levels in the BALF, and the collagen contents in the lung tissues in both *ghrl*^{-/-} mice and *ghsr*^{-/-} mice after BLM injection (Fig. 8, C–E, and Fig. 9, C–E).

Effects of hesperidin and glycyrrhizin administration on the BLM-induced ALI. We examined the effects of hesperidin and glycyrrhizin, both of which are components of RKT derived from *Aurantii nobilis pericarpium* and *Glycyrrhizae radix*, respectively (18, 42), on the BLM-induced ALI. Both hesperidin and glycyrrhizin administrations decreased the protein levels in the BALF after lung injury (Fig. 10, A and B).

DISCUSSION

In this study, we provide what is to our knowledge the first evidence of anti-inflammatory effects of RKT in an inflammatory disease model. Administration of RKT improved the BLM-induced weight loss, inhibited the induction of proinflammatory cytokines and chemokines, suppressed the recruitment of neutrophils into the alveolar spaces, protected AECs from lung injury, ameliorated lung fibrosis, and consequently

F10

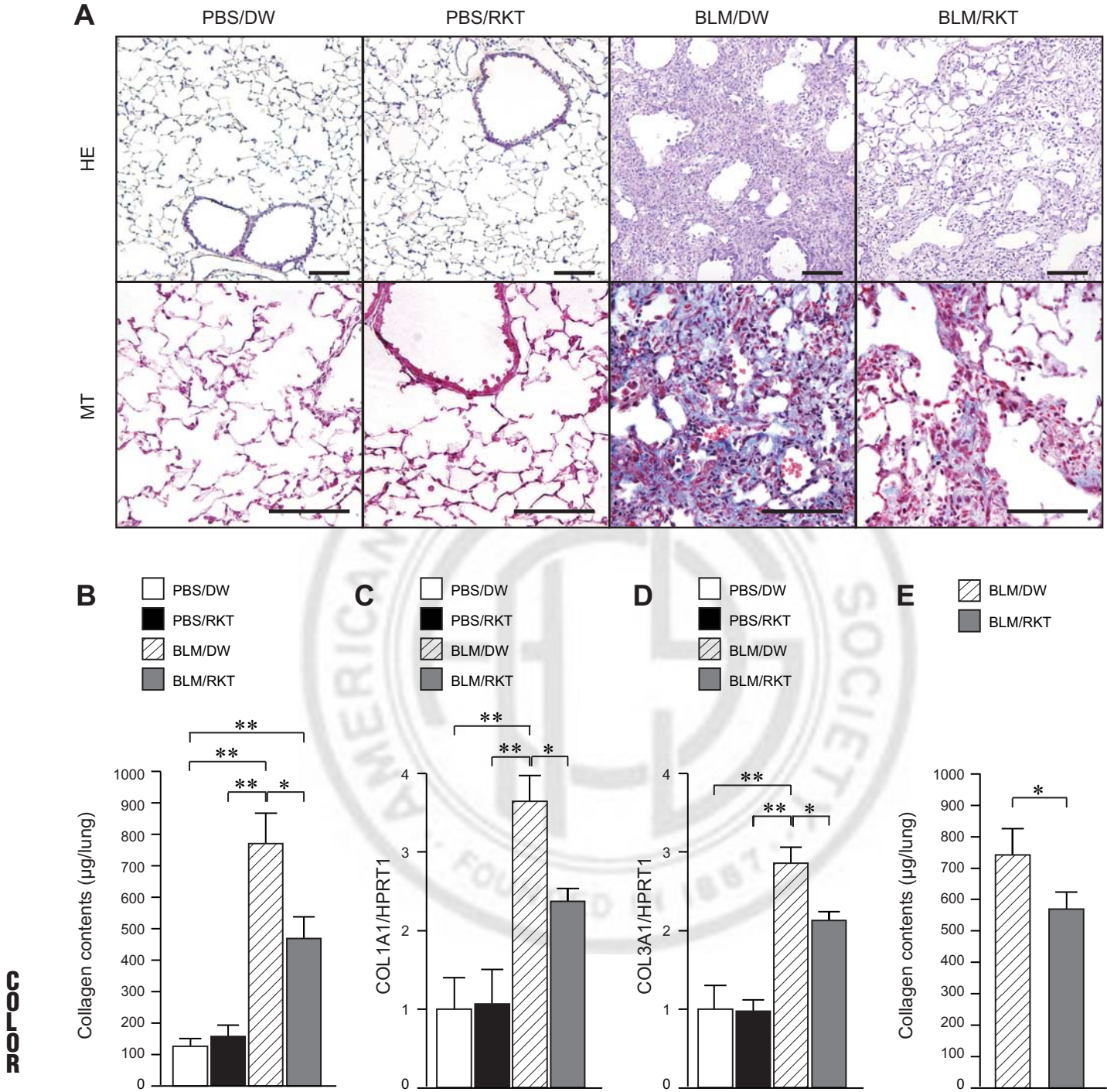


Fig. 4. Effects of RKT administration on pulmonary fibrosis in BLM-injected mice. *A*: representative HE staining (*top*) and Masson's trichrome (MT, *bottom*) staining of lung sections of PBS/DW, PBS/RKT, BLM/DW, and BLM/RKT mice at 14 days after the instillation of PBS or 6 U/kg of BLM. Data are representative lung sections from 5 mice per group. Scale bars: 100 µm. *B*: collagen contents in the lungs of PBS/DW, PBS/RKT, BLM/DW, and BLM/RKT mice at 14 days after the instillation of PBS or 6 U/kg of BLM. Data are means ± SE of 5–11 mice per group. **P* < 0.05; ***P* < 0.01. The mRNA levels of collagen type I alpha 1 (COL1A1) (*C*) and collagen type III alpha 1 (COL3A1) (*D*) in the whole lung lysates at 14 days after the administration of PBS or 6 U/kg of BLM. Results are expressed relative to the housekeeping gene HPRT1. Data are means ± SE of 3–11 mice per group. **P* < 0.05; ***P* < 0.01. *E*: effect of posttreatment of RKT in BLM-induced fibrosis. RKT or DW was given to BLM-injected mice daily during the 14-day study interval starting 7 days after 3 U/kg of BLM administration. Collagen contents in the lungs of BLM/DW and BLM/RKT mice at 21 days after BLM injection. Data are means ± SE of 8 mice per group. **P* < 0.05.

improved the survival rates after lung injury. We also demonstrated that RKT repressed the degradation of cytoplasmic IκB protein, the expressions of both phosphorylated NF-κB p65 and NF-κB p65 protein in the cytoplasm, and the nuclear

translocation of NF-κB. Although there are some clinical trials of RKT as a treatment for patients with dysfunction of the digestive tract (45, 46), there are no reports of clinical trials of RKT or its derivatives in ALI/ARDS patients. On the other

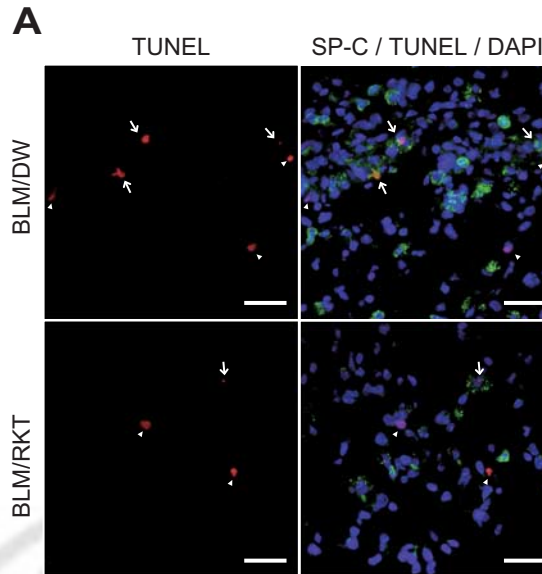
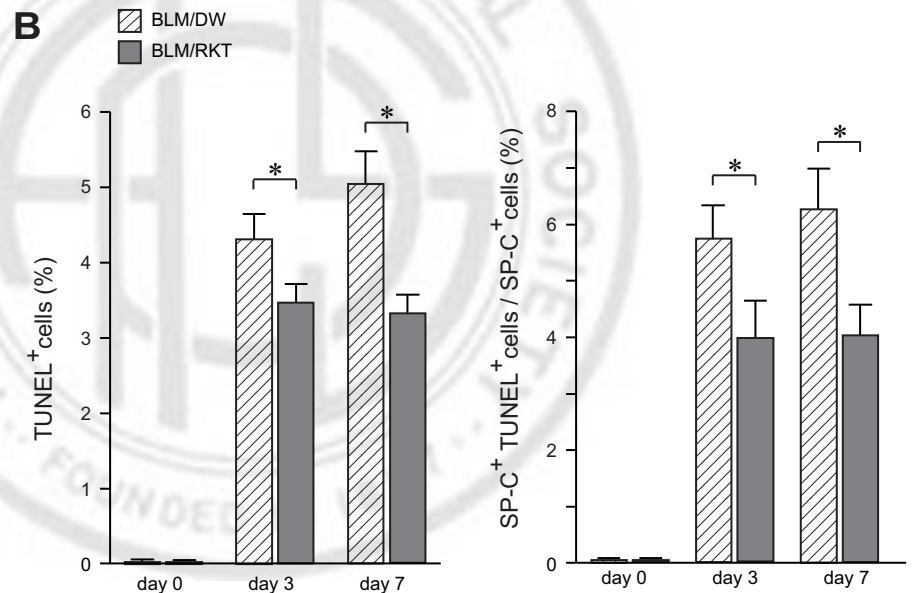


Fig. 5. Effect of RKT administration on cell apoptosis of alveolar epithelial cells in BLM-injected mice. *A*: representative profiles of immunostaining of surfactant protein-C (SP-C, green) and TUNEL staining (red) of lung sections of BLM/DW and BLM/RKT mice on *day 7* after the instillation of 6 U/kg of BLM. 4',6-diamidino-2-phenylindole (DAPI) was used in the counterstaining of the nucleus (blue). Numbers of both TUNEL-positive cells (arrowheads) and TUNEL and SP-C double-positive cells (arrows) were lower in the BLM/RKT lungs than the BLM/DW lungs. Scale bars: 25 μ m. *B*: quantification of TUNEL-positive cells and TUNEL and SP-C double-positive cells in BLM/DW and BLM/RKT lungs at *days 0, 3, and 7*. Ten high-power fields per slide were randomly selected, and the numbers of TUNEL-positive cells, SP-C-positive cells, and DAPI-positive cells were counted. Percentages of TUNEL-positive cells and TUNEL and SP-C double-positive cells were obtained by dividing the number of TUNEL-positive cells by the number of DAPI-positive cells and by dividing TUNEL and SP-C double-positive cells by SP-C positive cells. Data are means \pm SE of 5 mice per group. **P* < 0.05.



hand, hesperidin and glycyrrhizin, both of which are components of RKT, were studied in several clinical trials including those for rheumatoid arthritis (21), autoimmune hepatitis (59), and chronic hepatitis C (28). Our present results demonstrated the protective effects of RKT against BLM-induced ALI in mice. In regard to safety and tolerability, RKT, hesperidin, and glycyrrhizin administrations each had no severe side effects (21, 28, 45, 46, 59). We thus believe that RKT could provide a hopeful therapeutic strategy for ALI/ARDS.

Intratracheal administration of BLM induces lung injury via its ability to cause oxidant injury, DNA strand breakage, and the apoptosis of AECs, which leads to the induction of cytokines, chemokines and growth factors, the recruitment of inflammatory cells into lung parenchyma, and subsequent lung fibrosis (34). Our present findings showed that in BLM-injected mice, RKT administration significantly inhibited the

expressions of IL-1 β , TNF- α , IL-6, CXCL2/MIP-2, and TGF- β ₁, and reduced the alveolar infiltration of neutrophils. As does TNF- α , IL-1 β functions as a proinflammatory cytokine in response to tissue injury through the rapid induction of canonical IL-1 β target gene expressions including those of IL-6, CXCL2/MIP-2, and IL-1 β in multiple different cell types such as monocytes, epithelial cells, and endothelial cells (52). In response to ligand binding of the receptor, a complex sequence of combinatorial phosphorylation and ubiquitination events results in the activation of NF- κ B, a transcriptional factor that plays a crucial role in inflammatory signaling (12, 49, 52). Inducible NF- κ B activation depends on the phosphorylation-induced proteosomal degradation of the inhibitor of NF- κ B proteins (I κ Bs, such as I κ B α), which retain inactive NF- κ B dimers in the cytosol in unstimulated cells (11, 12). Previous studies have reported that the intratracheal administration of

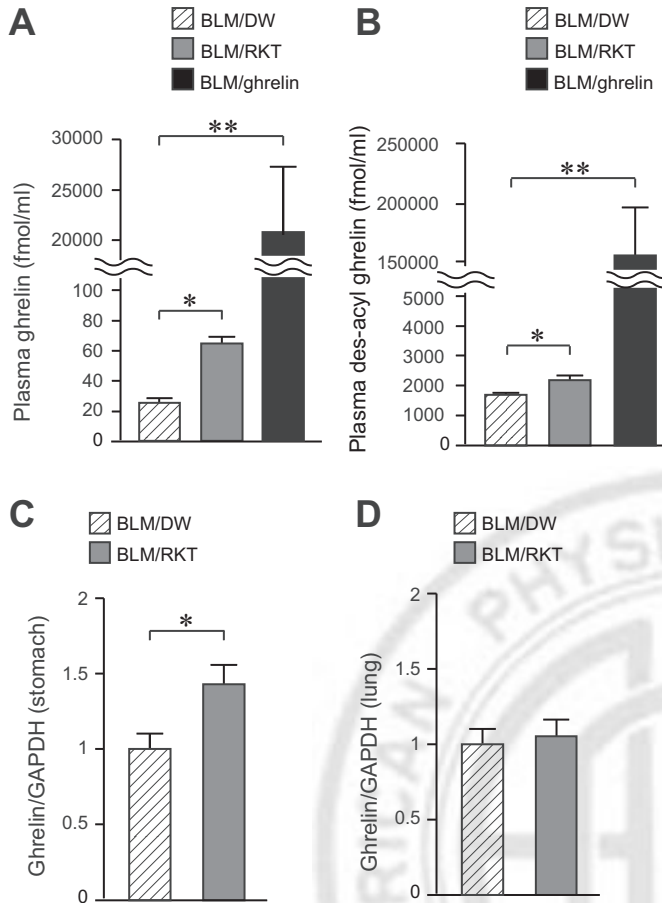


Fig. 6. Effect of RKT administration on induction of ghrelin in BLM-injected mice. Plasma levels of ghrelin (A) and des-acyl ghrelin (B) of BLM/DW mice ($n = 4$), BLM/RKT mice ($n = 6$), and BLM/ghrelin mice ($n = 4$) are shown. Data are means \pm SE. * $P < 0.05$; ** $P < 0.01$. Levels of expression of ghrelin mRNA in stomach (C) and lung (D) on day 14. Data are means \pm SE of 6 mice per group. * $P < 0.05$.

BLM induced the phosphorylation and degradation of I κ B α and the translocation of the active dimer of NF- κ B into the nucleus in the whole lungs of mice (10, 27). In the present study, we demonstrated the inhibitory effect of RKT administration on NF- κ B signaling through both the suppression of the expression levels of phosphorylated NF- κ B p65 and NF- κ B p65 protein in the cytoplasm and the retention of the cytosolic I κ B α protein levels in BLM-treated lungs. The blockage of the nuclear translocation of NF- κ B, as well as the suppression of IL-1 β expression, might reduce the induction of inflammatory cytokines and neutrophil alveolar infiltration in BLM-treated, RKT-administered mice.

The numbers of apoptotic AECs have been positively correlated with the levels of alveolar capillary barrier dysfunction, enhanced lung permeability, and subsequent lung scarring (3, 30). We showed here that the administration of RKT reduced the apoptosis of AECs in BLM-treated mice. The protective effect of RKT on AECs may prevent subsequent lung fibrosis by minimizing the denudation of the alveolar membrane, as well as by mitigating alveolar flooding. The reduction of neutrophil-mediated injury through a decrease in neutrophil alveolar accumulation may contribute to the protection of AECs in RKT-treated mice. In addition, RKT prevents cell

apoptosis in several types of epithelium. Previous studies demonstrated that RKT administration protected gastric parietal cells from drug-induced cytotoxicity (62). RKT administration also inhibited apoptosis of the small intestinal epithelial cells via the induction of the 60-kDa heat shock protein 60 (44). Another report showed an improvement in the epithelial barrier function of the esophageal mucosa after RKT treatment due to facilitation of the intracellular translocation of tight junction proteins (33). The direct protective mechanism of RKT against the injury of AECs merits further study.

The present study is the first report demonstrating the anti-fibrotic effect of RKT in injured lungs. In addition to RKT treatment starting 12 h after a BLM insult, the RKT treatment starting 7 days after BLM administration also ameliorated lung fibrosis. With regard to the mechanisms underlying the mitigation of lung fibrosis in RKT-treated mice, we observed a significant reduction of TGF- β and IL-1 β in the BALF and lung tissues of the BLM/RKT mice. Previous studies showed that an overexpression of TGF- β (24, 55) or IL-1 β (20) induced pulmonary fibrosis. RKT may therefore have an anti-fibrotic effect through the reduction of TGF- β and IL-1 β , in addition to its effect on the maintenance of an intact layer of AECs that suppresses fibroblast proliferation and matrix deposition. In addition, the RKT component glycyrrhizin was reported to suppress concanavalin A-induced liver fibrosis by regulating the CD4⁺ T cell response (47), a phenomenon that might also contribute to the amelioration of lung fibrosis in RKT-treated mice.

Our present data show that RKT administration significantly increased both the plasma ghrelin levels and mRNA expressions of ghrelin in the stomachs in BLM-injected WT mice. Several lines of evidence show that ghrelin has a direct suppressive effect on the production of proinflammatory cytokines in monocytes, T cells (7), endothelial cells (26), and AECs (14) through the activation of growth hormone secretagogue receptor (7, 26) or NF- κ B (26). In addition, we found earlier that ghrelin administration exerted a beneficial effect against BLM-induced ALI in mice by regulating lung inflammation (15). In the present study, unexpectedly, RKT administration also ameliorated lung inflammation and fibrosis and improved the survival rate in both *ghrl*^{-/-} mice and *ghsr*^{-/-} mice after lung injury. These results indicate that the protective effects of RKT on BLM-induced ALI were independent of the ghrelin signaling system.

With regard to the mechanisms of the anti-inflammatory effects of RKT against BLM-induced lung injury, we suspected that two components of RKT, hesperidin and glycyrrhizin, might directly mitigate lung inflammation in BLM-induced ALI. Hesperidin has been reported to have anti-inflammatory effects in several systems (8, 17), and it reduced the neutrophil activation and infiltration in a collagen-induced arthritis model (48). Another study reported that hesperidin suppressed inflammatory cell accumulation and decreased inflammatory mediators in the BALF of an ovalbumin-induced chronic airway inflammation model (53). Glycyrrhizin and its metabolite, 18 β -glycyrrhetic acid, have been reported to possess various pharmacological properties, including anti-inflammatory activity (16), antioxidative activity (25), and antifibrotic effects (35). Both glycyrrhizin and 18 β -glycyrrhetic acid exhibited anti-inflammatory activity through their inhibitory function against the conversion of hydrocortisone to

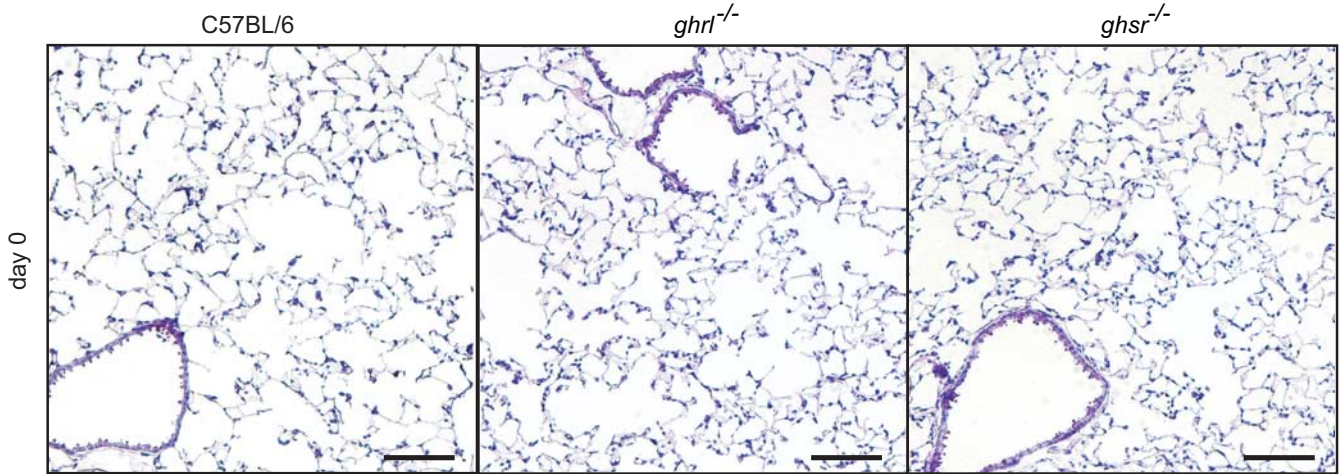


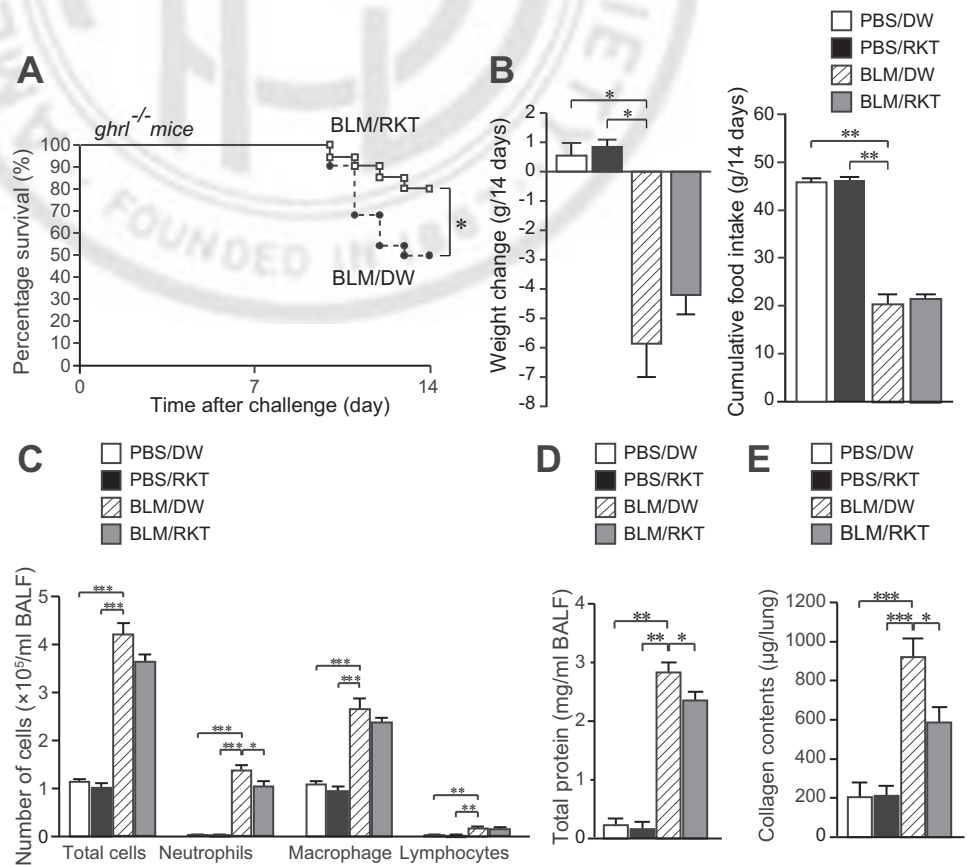
Fig. 7. HE staining of lung sections of C57BL/6 mice, ghrelin-deficient (*ghrl*^{-/-}) mice, and growth hormone secretagogue receptor-deficient (*ghsr*^{-/-}) mice at day 0. Representative HE staining of lung sections of PBS/DW group in C57BL/6 mice (left), *ghrl*^{-/-} mice (middle), and *ghsr*^{-/-} mice (right) at day 0 after treatment with PBS. The architecture of lungs in the *ghrl*^{-/-} mice and *ghsr*^{-/-} mice showed no difference from those of C57BL/6 mice. Data are representative lung sections from 5 mice per group. Scale bars: 100 μm.

its inactive metabolite cortisone (6, 40). It was also demonstrated that glycyrrhetic acid decreased ICAM-1 and macrophage inflammatory protein-1α expressions via the inactivation of NF-κB signaling (4, 58). In the present study, the administration of hesperidin or glycyrrhizin decreased the alveolar permeability solely in the BLM-treated mice. These data suggest that the anti-inflammatory effects of RKT in BLM-induced ALI might be, at least in part, dependent on the

direct effects of hesperidin and glycyrrhizin. The reports that hesperidin or glycyrrhizin administration mitigated LPS-induced ALI in mice (25, 38, 61) support this idea.

In regard to the mechanisms of the orexigenic effects of RKT, in contrast to the anti-inflammatory effects, the administration of RKT did not decrease the degree of loss of body weight and food intake reduction in the *ghrl*^{-/-} mice or the *ghsr*^{-/-} mice. These findings suggested that the mitigative

Fig. 8. Effects of RKT administration on BLM-induced acute lung injury in ghrelin-deficient mice. **A:** Kaplan-Meier survival curves for the BLM/DW group (dashed line, *n* = 22) and BLM/RKT group (solid line, *n* = 21) in ghrelin-deficient (*ghrl*^{-/-}) mice for 14 days after challenge with 6 U/kg of BLM. **P* < 0.05. **B:** alterations in body weight (left) and cumulative food intake (right) over 14 days after the instillation of 6 U/kg of BLM or PBS in *ghrl*^{-/-} mice (PBS/DW *n* = 7, PBS/RKT *n* = 7, BLM/DW *n* = 10, BLM/RKT *n* = 16). Data are means ± SE. **P* < 0.05; ***P* < 0.01. **C:** Cell counts (C) and total protein concentrations (D) in the BALF of DW- or RKT-administered *ghrl*^{-/-} mice 7 days after the instillation of PBS or 6 U/kg of BLM. Data are means ± SE of 3–10 (C) and 4–8 (D) mice per group. **P* < 0.05; ***P* < 0.01; ****P* < 0.001. **E:** collagen contents in the lungs of PBS/DW, PBS/RKT, BLM/DW and BLM/RKT *ghrl*^{-/-} mice at 14 days after the instillation of PBS or 6 U/kg of BLM. Data are means ± SE of 4–11 mice per group. **P* < 0.05; ****P* < 0.001.



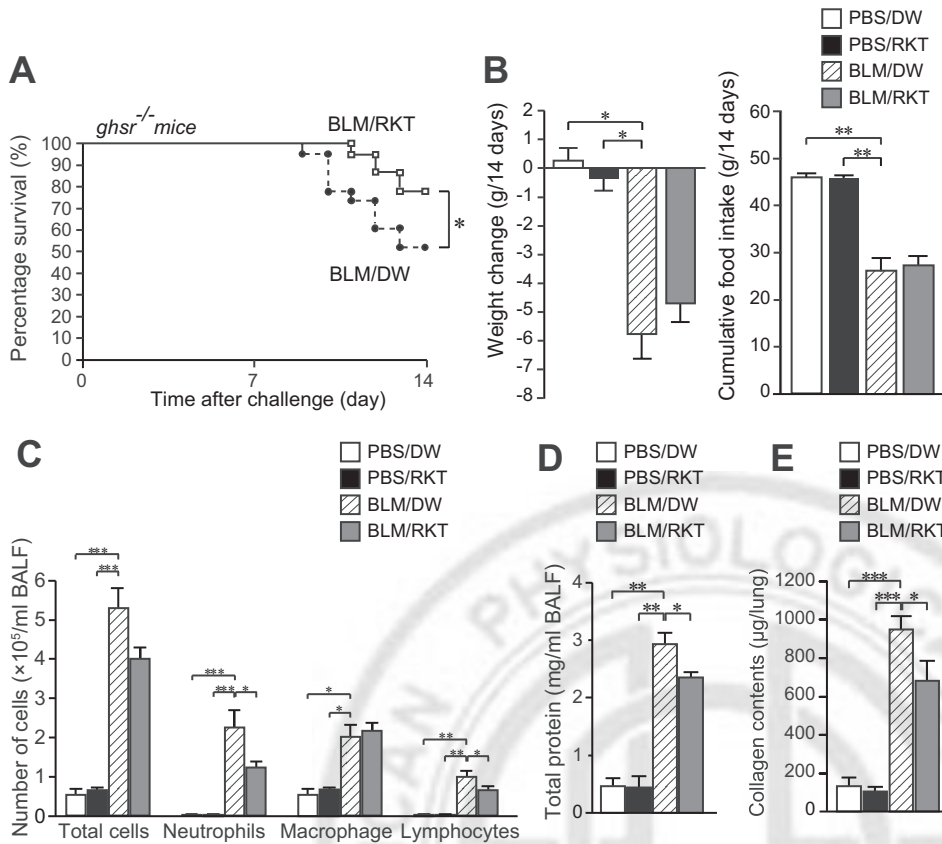


Fig. 9. Effects of RKT administration on BLM-induced acute lung injury in growth hormone secretagogue receptor-deficient mice. **A**: Kaplan-Meier survival curves for the BLM/DW group (dashed line, *n* = 23) and BLM/RKT group (solid line, *n* = 23) in growth hormone secretagogue receptor-deficient (*ghsr*^{-/-}) mice for 14 days after challenge with 6 U/kg of BLM. **P* < 0.05. **B**: alterations in body weight (left) and cumulative food intake (right) over 14 days after the instillation of 6 U/kg of BLM or PBS in *ghsr*^{-/-} mice (PBS/DW *n* = 5, PBS/RKT *n* = 5, BLM/DW *n* = 12, BLM/RKT *n* = 18). Data are means ± SE. **P* < 0.05; ***P* < 0.01. **C**: Cell counts (C) and total protein concentrations (D) in the BALF of DW- or RKT-administered *ghsr*^{-/-} mice 7 days after the instillation of PBS or 6 U/kg of BLM. Data are means ± SE of 3–11 (C) and 3–13 (D) mice per group. **P* < 0.05; ***P* < 0.01; ****P* < 0.001. **E**: collagen contents in the lungs of PBS/DW, PBS/RKT, BLM/DW, and BLM/RKT *ghsr*^{-/-} mice at 14 days after the instillation of PBS or 6 U/kg of BLM. Data are means ± SE of 5–12 mice per group. **P* < 0.05; ****P* < 0.001.

effects of RKT on the food intake reduction in BLM-injected mice were dependent on the ghrelin system. The previous finding that the suppressive effect of RKT against cisplatin-induced anorexia was blocked by a ghrelin antagonist (43) supports our findings. The precise mechanism underlying how RKT exerts its physiological effects in a ghrelin-dependent or ghrelin-independent manner according to the type of action needs to be examined in future studies.

In this study, both the *ghrl*^{-/-} mice and the *ghsr*^{-/-} mice demonstrated higher numbers of total cells and macrophages in the BALF after injury compared with the wild-type mice. These data indicated that the lack of an endogenous ghrelin signaling system might induce increased macrophage infiltration into the alveolar spaces after lung injury. Regarding the mechanisms of aggravated macrophage infiltration in the lungs in *ghrl*^{-/-} mice and the *ghsr*^{-/-} mice, a previous study

demonstrated the existence of both growth hormone secretagogue receptor (GHS-R) and ghrelin expressions in human peripheral blood mononuclear cells (PBMCs), and ghrelin acts via GHS-R to specifically inhibit the expression of proinflammatory cytokines including TNF-α in the PBMCs (7). Another study showed that ghrelin treatment downregulated the production of TNF-α by LPS-stimulated RAW264.7 cells (5). Since TNF-α is the key cytokine that activates the cell properties of macrophages, such as migration (50) and the secretion of proinflammatory cytokines (36), the increases in the number of macrophages in the BALF of the *ghrl*^{-/-} mice and *ghsr*^{-/-} mice after injury in the present study might be due to the lack of an endogenous ghrelin signaling system in the macrophages.

We previously reported that ghrelin treatment significantly improved the survival rate of BLM-induced ALI (15). In the present study, in ghrelin-treated WT mice, we found a 1,000-

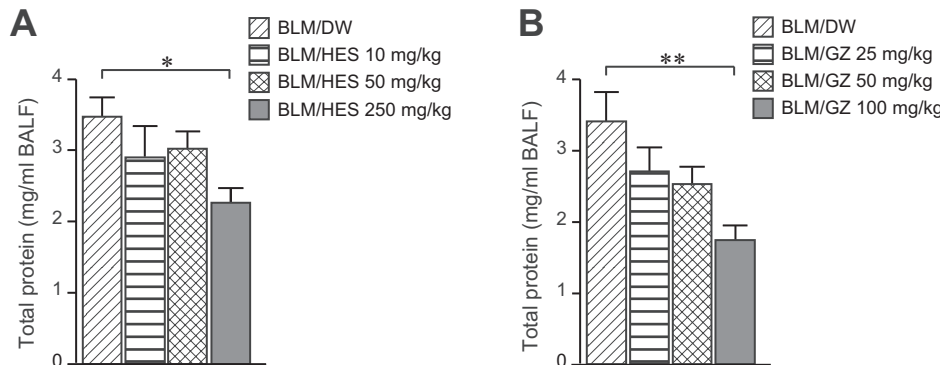


Fig. 10. Effects of HES and GZ on the vascular permeability in the lungs of BLM-injected mice. Total protein concentrations in the BALF of DW-, HES (10, 50, or 250 mg/kg, A), and GZ (25, 50, or 100 mg/kg, B)-administered mice 7 days after 6 U/kg of BLM instillation. Data are means ± SE of 7–8 (A) and 7 (B) mice per group. **P* < 0.05; ***P* < 0.01.

fold increase in the plasma ghrelin level compared with the DW-treated WT mice after lung injury. We also observed comparable survival rates of BLM/DW *ghrl*^{-/-} mice, BLM/DW *ghsr*^{-/-} mice, and BLM/DW WT mice. Overall, we surmise that the lack of endogenous expressions of ghrelin and GHS-R might not influence the differences in the survival rates of mice with a BLM-induced acute lung injury, and we consider that a pharmacological dose of ghrelin administration that leads to overwhelming higher plasma ghrelin levels compared with the endogenous plasma ghrelin levels is necessary for the improvement of survival rates in BLM-injected mice.

In summary, our results demonstrated the efficacy of RKT administration in a rodent model of ALI. RKT administration protected AECs from injury, reduced lung inflammation, ameliorated lung fibrosis, and ultimately saved mice from BLM-induced ALI. The pleiotropic effects of RKT against ALI shown in this study suggest a novel and attractive therapeutic strategy for the treatment of ALI in humans.

ACKNOWLEDGMENTS

We thank Kahori Miyoshi, Koji Toshinai, Sumie Tajiri, and Miki Oshikawa (Miyazaki University) for technical support.

GRANTS

This work was supported in part by a Grant-in-Aid for Scientific Research (no. 24591171); a Grant-in-Aid for challenging Exploratory Research (no. 24659406); a grant from the Ministry of Education, Culture, Sports, Science and Technology (MEXT), a Health and Labour Sciences Research Grant for Clinical Research Translational Research General (no. 002); a grant from the Japan Intractable Diseases Research Foundation; and a grant from Tsumura and Co.

DISCLOSURES

S.M., C.Y., S.I., and T.H. are employed by Tsumura and Co. H.T., S.Y., A.M., and N.M. declare that there were no conflicts of interest.

AUTHOR CONTRIBUTIONS

H.T., S.Y., T.H., and M.N. conception and design of research; H.T., A.M., S.I., S.M., and C.Y. performed experiments; H.T. analyzed data; H.T., S.Y., S.I., T.H., and M.N. interpreted results of experiments; H.T. prepared figures; H.T., S.Y., and M.N. drafted manuscript; H.T., S.Y., and M.N. edited and revised manuscript; H.T., S.Y., and M.N. approved final version of manuscript.

REFERENCES

- Aghanouri R, Ghanei M, Aslani J, Keivani-Amine H, Rastegar F, Karkhane A. Fibrogenic cytokine levels in bronchoalveolar lavage aspirates 15 years after exposure to sulfur mustard. *Am J Physiol Lung Cell Mol Physiol* 287: L1160–L1164, 2004.
- Baldanzi G, Filigheddu N, Cutrupi S, Catapano F, Bonisconi S, Fubini A, Malan D, Baj G, Granata R, Broglio F, Papotti M, Surico N, Bussolino F, Isgaard J, Deghenghi R, Sinigaglia F, Prat M, Muccioli G, Ghigo E, Graziani A. Ghrelin and des-acyl ghrelin inhibit cell death in cardiomyocytes and endothelial cells through ERK1/2 and PI 3-kinase/AKT. *J Cell Biol* 159: 1029–1037, 2002.
- Bao S, Knoell DL. Zinc modulates cytokine-induced lung epithelial cell barrier permeability. *Am J Physiol Lung Cell Mol Physiol* 291: L1132–L1141, 2006.
- Chang YL, Chen CL, Kuo CL, Chen BC, You JS. Glycyrrhetic acid inhibits ICAM-1 expression via blocking JNK and NF-kappaB pathways in TNF-alpha-activated endothelial cells. *Acta Pharmacol Sin* 31: 546–553, 2010.
- Chorny A, Anderson P, Gonzalez-Rey E, Delgado M. Ghrelin protects against experimental sepsis by inhibiting high-mobility group box 1 release and by killing bacteria. *J Immunol* 180: 8369–8377, 2008.
- Classen-Houben D, Schuster D, Da Cunha T, Odermatt A, Wolber G, Jordis U, Kueenburb B. Selective inhibition of 11beta-hydroxysteroid dehydrogenase 1 by 18alpha-glycyrrhetic acid but not 18beta-glycyrrhetic acid. *J Steroid Biochem Mol Biol* 113: 248–252, 2009.
- Dixit VD, Schaffer EM, Pyle RS, Collins GD, Sakthivel SK, Palaniappan R, Lillard JW Jr, Taub DD. Ghrelin inhibits leptin- and activation-induced proinflammatory cytokine expression by human monocytes and T cells. *J Clin Invest* 114: 57–66, 2004.
- Emim JA, Oliveira AB, Lapa AJ. Pharmacological evaluation of the anti-inflammatory activity of a citrus bioflavonoid, hesperidin, and the isoflavonoids, dauricin and claussequinone, in rats and mice. *J Pharm Pharmacol* 46: 118–122, 1994.
- Erickson SE, Martin GS, Davis JL, Matthay MA, Eisner MD. Recent trends in acute lung injury mortality: 1996–2005. *Crit Care Med* 37: 1574–1579, 2009.
- Gurujeyalakshmi G, Wang Y, Giri SN. Taurine and niacin block lung injury and fibrosis by down-regulating bleomycin-induced activation of transcription nuclear factor-kappaB in mice. *J Pharmacol Exp Ther* 293: 82–90, 2000.
- Hayden MS, Ghosh S. Shared principles in NF-kappaB signaling. *Cell* 132: 344–362, 2008.
- Henkel T, Machleidt T, Alkalay I, Kronke M, Ben-Neriah Y, Baeuerle PA. Rapid proteolysis of I kappa B-alpha is necessary for activation of transcription factor NF-kappa B. *Nature* 365: 182–185, 1993.
- Horvath TL, Diano S, Sotonyi P, Heiman M, Tschop M. Minireview: ghrelin and the regulation of energy balance—a hypothalamic perspective. *Endocrinology* 142: 4163–4169, 2001.
- Hou Y, An J, Hu XR, Sun BB, Lin J, Xu D, Wang T, Wen FQ. Ghrelin inhibits interleukin-8 production induced by hydrogen peroxide in A549 cells via NF-kappaB pathway. *Int Immunopharmacol* 9: 120–126, 2009.
- Imazu Y, Yanagi S, Miyoshi K, Tsubouchi H, Yamashita S, Matsumoto N, Ashitani J, Kangawa K, Nakazato M. Ghrelin ameliorates bleomycin-induced acute lung injury by protecting alveolar epithelial cells and suppressing lung inflammation. *Eur J Pharmacol* 672: 153–158, 2011.
- Ishida T, Mizushima Y, Yagi S, Irino Y, Nishiumi S, Miki I, Kondo Y, Mizuno S, Yoshida H, Azuma T, Yoshida M. Inhibitory effects of glycyrrhetic acid on DNA polymerase and inflammatory activities. *Evid Based Complement Alternat Med* 2012: 650514, 2012.
- Jain M, Parmar HS. Evaluation of antioxidative and anti-inflammatory potential of hesperidin and naringin on the rat air pouch model of inflammation. *Inflamm Res* 60: 483–491, 2011.
- Kido T, Nakai Y, Kase Y, Sakakibara I, Nomura M, Takeda S, Aburada M. Effects of rikkunshi-to, a traditional Japanese medicine, on the delay of gastric emptying induced by N(G)-nitro-L-arginine. *J Pharm Sci* 98: 161–167, 2005.
- Kojima M, Hosoda H, Date Y, Nakazato M, Matsuo H, Kangawa K. Ghrelin is a growth-hormone-releasing acylated peptide from stomach. *Nature* 402: 656–660, 1999.
- Kolb M, Margetts PJ, Anthony DC, Pitossi F, Gauldie J. Transient expression of IL-1beta induces acute lung injury and chronic repair leading to pulmonary fibrosis. *J Clin Invest* 107: 1529–1536, 2001.
- Kometani T, Fukuda T, Kakuma T, Kawaguchi K, Tamura W, Kumazawa Y, Nagata K. Effects of alpha-glucosylhesperidin, a bioactive food material, on collagen-induced arthritis in mice and rheumatoid arthritis in humans. *Immunopharmacol Immunotoxicol* 30: 117–134, 2008.
- Kusunoki H, Haruma K, Hata J, Ishii M, Kamada T, Yamashita N, Honda K, Inoue K, Imamura H, Manabe N, Shiotani A, Tsunoda T. Efficacy of rikkunshito, a traditional Japanese medicine (kampo), in treating functional dyspepsia. *Intern Med* 49: 2195–2202, 2010.
- Lareu RR, Zeugolis DI, Abu-Rub M, Pandit A, Raghunath M. Essential modification of the Sircol Collagen Assay for the accurate quantification of collagen content in complex protein solutions. *Acta Biomater* 6: 3146–3151, 2010.
- Lee CG, Homer RJ, Zhu Z, Lanone S, Wang X, Kotliansky V, Shipley JM, Gotwals P, Noble P, Chen Q, Senior RM, Elias JA. Interleukin-13 induces tissue fibrosis by selectively stimulating and activating transforming growth factor beta(1). *J Exp Med* 194: 809–821, 2001.
- Lee CS, Kim YJ, Han ES. Glycyrrhizin protection against 3-morpholino-synthonime-induced mitochondrial dysfunction and cell death in lung epithelial cells. *Life Sci* 80: 1759–1767, 2007.
- Li WG, Gavrilu D, Liu X, Wang L, Gunnlaugsson S, Stoll LL, McCormick ML, Sigmund CD, Tang C, Weintraub NL. Ghrelin inhibits proinflammatory responses and nuclear factor-kappaB activation in human endothelial cells. *Circulation* 109: 2221–2226, 2004.

27. Ma Y, Wang M, Li N, Wu R, Wang X. Bleomycin-induced nuclear factor-kappaB activation in human bronchial epithelial cells involves the phosphorylation of glycogen synthase kinase 3beta. *Toxicol Lett* 187: 194–200, 2009.
28. Manns MP, Wedemeyer H, Singer A, Khomutjanskaja N, Dienes HP, Roskams T, Goldin R, Hehnke U, Inoue H. Glycyrrhizin in patients who failed previous interferon alpha-based therapies: biochemical and histological effects after 52 weeks. *J Viral Hepat* 19: 537–546, 2012.
29. Matsumura T, Arai M, Yonemitsu Y, Maruoka D, Tanaka T, Suzuki T, Yoshikawa M, Imazeki F, Yokosuka O. The traditional Japanese medicine Rikkunshito increases the plasma level of ghrelin in humans and mice. *J Gastroenterol* 45: 300–307, 2010.
30. Matthay MA, Ware LB, Zimmerman GA. The acute respiratory distress syndrome. *J Clin Invest* 122: 2731–2740, 2012.
31. Matthay MA, Zemans RL. The acute respiratory distress syndrome: pathogenesis and treatment. *Annu Rev Pathol* 6: 147–163, 2011.
32. Matute-Bello G, Frevert CW, Martin TR. Animal models of acute lung injury. *Am J Physiol Lung Cell Mol Physiol* 295: L379–L399, 2008.
33. Miwa H, Koseki J, Oshima T, Kondo T, Tomita T, Watari J, Matsumoto T, Hattori T, Kubota K, Iizuka S. Rikkunshito, a traditional Japanese medicine, may relieve abdominal symptoms in rats with experimental esophagitis by improving the barrier function of epithelial cells in esophageal mucosa. *J Gastroenterol* 45: 478–487, 2010.
34. Moore BB, Hogaboam CM. Murine models of pulmonary fibrosis. *Am J Physiol Lung Cell Mol Physiol* 294: L152–L160, 2008.
35. Moro T, Shimoyama Y, Kushida M, Hong YY, Nakao S, Higashiyama R, Sugioka Y, Inoue H, Okazaki I, Inagaki Y. Glycyrrhizin and its metabolite inhibit Smad3-mediated type I collagen gene transcription and suppress experimental murine liver fibrosis. *Life Sci* 83: 531–539, 2008.
36. Mosser DM, Edwards JP. Exploring the full spectrum of macrophage activation. *Nat Rev Immunol* 8: 958–969, 2008.
37. Nakazato M, Murakami N, Date Y, Kojima M, Matsuo H, Kangawa K, Matsukura S. A role for ghrelin in the central regulation of feeding. *Nature* 409: 194–198, 2001.
38. Ni YF, Kuai JK, Lu ZF, Yang GD, Fu HY, Wang J, Tian F, Yan XL, Zhao YC, Wang YJ, Jiang T. Glycyrrhizin treatment is associated with attenuation of lipopolysaccharide-induced acute lung injury by inhibiting cyclooxygenase-2 and inducible nitric oxide synthase expression. *J Surg Res* 165: e29–e35, 2011.
39. Sato T, Kurokawa M, Nakashima Y, Ida T, Takahashi T, Fukue Y, Ikawa M, Okabe M, Kangawa K, Kojima M. Ghrelin deficiency does not influence feeding performance. *Regul Pept* 145: 7–11, 2008.
40. Schleimer RP. Potential regulation of inflammation in the lung by local metabolism of hydrocortisone. *Am J Respir Cell Mol Biol* 4: 166–173, 1991.
41. Sun Y, Wang P, Zheng H, Smith RG. Ghrelin stimulation of growth hormone release and appetite is mediated through the growth hormone secretagogue receptor. *Proc Natl Acad Sci USA* 101: 4679–4684, 2004.
42. Takeda H, Muto S, Hattori T, Sadakane C, Tsuchiya K, Katsurada T, Ohkawara T, Oridate N, Asaka M. Rikkunshito ameliorates the aging-associated decrease in ghrelin receptor reactivity via phosphodiesterase III inhibition. *Endocrinology* 151: 244–252, 2010.
43. Takeda H, Sadakane C, Hattori T, Katsurada T, Ohkawara T, Nagai K, Asaka M. Rikkunshito, an herbal medicine, suppresses cisplatin-induced anorexia in rats via 5-HT2 receptor antagonism. *Gastroenterology* 134: 2004–2013, 2008.
44. Tamaki K, Otaka M, Shibuya T, Sakamoto N, Yamamoto S, Odashima M, Itoh H, Watanabe S. Traditional herbal medicine, rikkunshito, induces HSP60 and enhances cytoprotection of small intestinal mucosal cells as a nontoxic chaperone inducer. *Evid Based Complement Alternat Med* 2012: 278958, 2012.
45. Tokashiki R, Okamoto I, Funato N, Suzuki M. Rikkunshito improves globus sensation in patients with proton-pump inhibitor-refractory laryngopharyngeal reflux. *World J Gastroenterol* 19: 5118–5124, 2013.
46. Tominaga K, Iwakiri R, Fujimoto K, Fujiwara Y, Tanaka M, Shimoyama Y, Umegaki E, Higuchi K, Kusano M, Arakawa T. Rikkunshito improves symptoms in PPI-refractory GERD patients: a prospective, randomized, multicenter trial in Japan. *J Gastroenterol* 47: 284–292, 2012.
47. Tu CT, Li J, Wang FP, Li L, Wang JY, Jiang W. Glycyrrhizin regulates CD4+T cell response during liver fibrogenesis via JNK, ERK and PI3K/AKT pathway. *Int Immunopharmacol* 14: 410–421, 2012.
48. Umar S, Kumar A, Sajad M, Zargan J, Ansari M, Ahmad S, Katiyar CK, Khan HA. Hesperidin inhibits collagen-induced arthritis possibly through suppression of free radical load and reduction in neutrophil activation and infiltration. *Rheumatol Int* 33: 657–663, 2013.
49. Vaillancourt F, Morquette B, Shi Q, Fahmi H, Lavigne P, Di Battista JA, Fernandes JC, Benderdour M. Differential regulation of cyclooxygenase-2 and inducible nitric oxide synthase by 4-hydroxynonenal in human osteoarthritic chondrocytes through ATF-2/CREB-1 transactivation and concomitant inhibition of NF-kappaB signaling cascade. *J Cell Biochem* 100: 1217–1231, 2007.
50. Wang J, Tian Y, Phillips KL, Chiverton N, Haddock G, Bunning RA, Cross AK, Shapiro IM, Le Maitre CL, Risbud MV. Tumor necrosis factor alpha- and interleukin-1beta-dependent induction of CCL3 expression by nucleus pulposus cells promotes macrophage migration through CCR1. *Arthritis Rheum* 65: 832–842, 2013.
51. Ware LB, Matthay MA. The acute respiratory distress syndrome. *N Engl J Med* 342: 1334–1349, 2000.
52. Weber A, Wasiliew P, Kracht M. Interleukin-1 (IL1) pathway. *Sci Signal* 3: cm1, 2010.
53. Wei D, Ci X, Chu X, Wei M, Hua S, Deng X. Hesperidin suppresses ovalbumin-induced airway inflammation in a mouse allergic asthma model. *Inflammation* 35: 114–121, 2012.
54. Wiener-Kronish JP, Albertine KH, Matthay MA. Differential responses of the endothelial and epithelial barriers of the lung in sheep to Escherichia coli endotoxin. *J Clin Invest* 88: 864–875, 1991.
55. Wilson MS, Madala SK, Ramalingam TR, Gochuico BR, Rosas IO, Cheever AW, Wynn TA. Bleomycin and IL-1beta-mediated pulmonary fibrosis is IL-17A dependent. *J Exp Med* 207: 535–552, 2010.
56. World Health Organization. *WHO Guidelines on Good Agricultural and Collection Practices (GACP) for Medicinal Plants*. Geneva: World Health Organization, 2003.
57. Wu R, Dong W, Zhou M, Zhang F, Marini CP, Ravikumar TS, Wang P. Ghrelin attenuates sepsis-induced acute lung injury and mortality in rats. *Am J Respir Crit Care Med* 176: 805–813, 2007.
58. Xiao Y, Xu J, Mao C, Jin M, Wu Q, Zou J, Gu Q, Zhang Y, Zhang Y. 18Beta-glycyrrhetic acid ameliorates acute Propionibacterium acnes-induced liver injury through inhibition of macrophage inflammatory protein-1alpha. *J Biol Chem* 285: 1128–1137, 2010.
59. Yasui S, Fujiwara K, Tawada A, Fukuda Y, Nakano M, Yokosuka O. Efficacy of intravenous glycyrrhizin in the early stage of acute onset autoimmune hepatitis. *Dig Dis Sci* 56: 3638–3647, 2011.
60. Yasukawa K, Yu SY, Kakinuma S, Takido M. Inhibitory effect of rikkunshito, a traditional Chinese herbal prescription, on tumor promotion in two-stage carcinogenesis in mouse skin. *Biol Pharm Bull* 18: 730–733, 1995.
61. Yeh CC, Kao SJ, Lin CC, Wang SD, Liu CJ, Kao ST. The immunomodulation of endotoxin-induced acute lung injury by hesperidin in vivo and in vitro. *Life Sci* 80: 1821–1831, 2007.
62. Yu XM, Liu YZ, Noda T, Ogawa K. Chinese traditional medicine protects gastric parietal cells from adriamycin cytotoxicity. *Acta Histochem Cytochem* 28: 539–547, 1995.